Interplay between total thickness and period thickness in the phonon thermal conductivity of superlattices from the nanoscale to the microscale: Coherent versus incoherent phonon transport

Ramez Cheaito, Carlos A. Polanco, Sadhvikas Addamane, Jingjie Zhang, Avik W. Ghosh, Ganesh Balakrishnan, and Patrick E. Hopkins

Phys. Rev. B **97**, 085306 — Published 20 February 2018

DOI: 10.1103/PhysRevB.97.085306

Interplay between total thickness and period thickness in the phonon thermal conductivity of superlattices across nano-to-microscales: Coherent vs. incoherent phonon transport

Ramez Cheaito,[1] Carlos A. Polanco,[2] Sadhvikas Addamane,[3] Jingjie Zhang,[2]
Avik W. Ghosh,[2] Ganesh Balakrishnan,[3] and Patrick E. Hopkins[1,4,5,*]

[1]*Department of Mechanical and Aerospace Engineering, University of Virginia, Charlottesville, Virginia 22904, USA*
[2]*Department of Electrical and Computer Engineering, University of Virginia, Charlottesville, Virginia 22904, USA*
[3]*Department of Electrical and Computer Engineering, University of New Mexico, Albuquerque, New Mexico 87106, USA*
[4]*Department of Materials Science and Engineering, University of Virginia, Charlottesville, Virginia 22904, USA*
[5]*Department of Physics, University of Virginia, Charlottesville, Virginia 22904, USA*

We report on the room temperature thermal conductivity of AlAs-GaAs superlattices (SLs), in which we systematically vary the period thickness and total thickness between 2 − 24 nm and 20.1 − 2,160 nm, respectively. The thermal conductivity increases with the SL thickness and plateaus at a thickness around 200 nm, showing a clear transition from a quasi-ballistic to a diffusive phonon transport regime. These results demonstrate the existence of classical size effects in SLs, even at the highest interface density samples. We use harmonic Atomistic Green's function calculations to capture incoherence in phonon transport by averaging the calculated transmission over several purely coherent simulations of independent SL with different random mixing at the AlAs-GaAs interfaces. These simulations demonstrate the significant contribution of incoherent phonon transport through the decrease in the transmission and conductance in the SLs as the number of interfaces increases. In spite of this conductance decrease, our simulations show a quasilinear increase in thermal conductivity with the superlattice thickness. This suggests that the observation of a quasilinear increase in thermal conductivity can have important contributions from incoherent phonon transport. Furthermore, this seemingly linear slope in thermal conductivity vs. SL thickness data may actually be non-linear when extended to a larger number of periods, which is a signature of incoherent effects. Indeed, this trend for superlattices with interatomic mixing at the interfaces could easily be interpreted as linear when the number of periods is small. Our results reveal that the change in thermal conductivity with period thickness is dominated by incoherent (particlelike) phonons, whose properties are not dictated by changes in the AlAs or GaAs phonon dispersion relations. This work demonstrates the importance of studying both period and sample thickness dependencies of thermal conductivity to understand the relative contributions of coherent and incoherent phonon transport in the thermal conductivity in SLs.

I. INTRODUCTION

Superlattices represent a group of metamaterials that have attracted considerable attention over the past few decades due to their promise as material solutions in thermoelectric devices[1,2] and applications in quantum cascade[3] and vertical cavity surface emitting lasers.[4] In addition to the vast application space of superlattices (SLs), these nanostructures provide a means to test for the existence of coherent phonons, or when the phase difference between two spatio-temporal points of a vibrational wave remain constant.[5–8] For SLs, two length scales affect thermal transport: long range and short range boundary scattering. Long range boundary scattering occurs when phonons with mean free paths (mfp) of the order of the superlattice thickness, L, scatter at the sample boundary. Short range boundary scattering takes place when phonons with mfps of the order of the superlattice period thickness, d_{SL}, scatter at the internal interfaces. The interplay between phonon scattering at period boundaries and sample boundaries is not fully understood,[9] partially due to discrepancies in literature data on thermal conductivity of SLs (κ_{SL}).

To illustrate this problem, we motivate with two material system SL examples: aluminum arsenide-gallium arsenide (AlAs-GaAs) and silicon-germanium (Si-Ge) SLs, both of which have been extensively studied.[6,10–16] Figure 1 summarizes literature thermal conductivity data on various AlAs-GaAs and Si-Ge superlattice systems plotted versus d_{SL} in Fig. 1A and 1C and versus L in Fig. 1B and 1D. For AlAs-GaAs SLs, Luckyanova *et al.*[6] reported a linear increase in κ_{SL} as a function of L. However, the study limited the total thickness to a maximum of 216 nm and the period thickness to 24 nm, and thus could not study the effects of smaller d_{SL} and larger L on phonon transport. Capinski *et al.*[10] studied AlAs-GaAs SLs where the period thickness and total thickness varied simultaneously. In contrast to Luckyanova's data, their data did not show any clear trend with L. For Si-Ge SLs, a more pronounced discrepancy can be observed. While Borca-Tasciuc *et al.*[12] reported a decrease in ther-

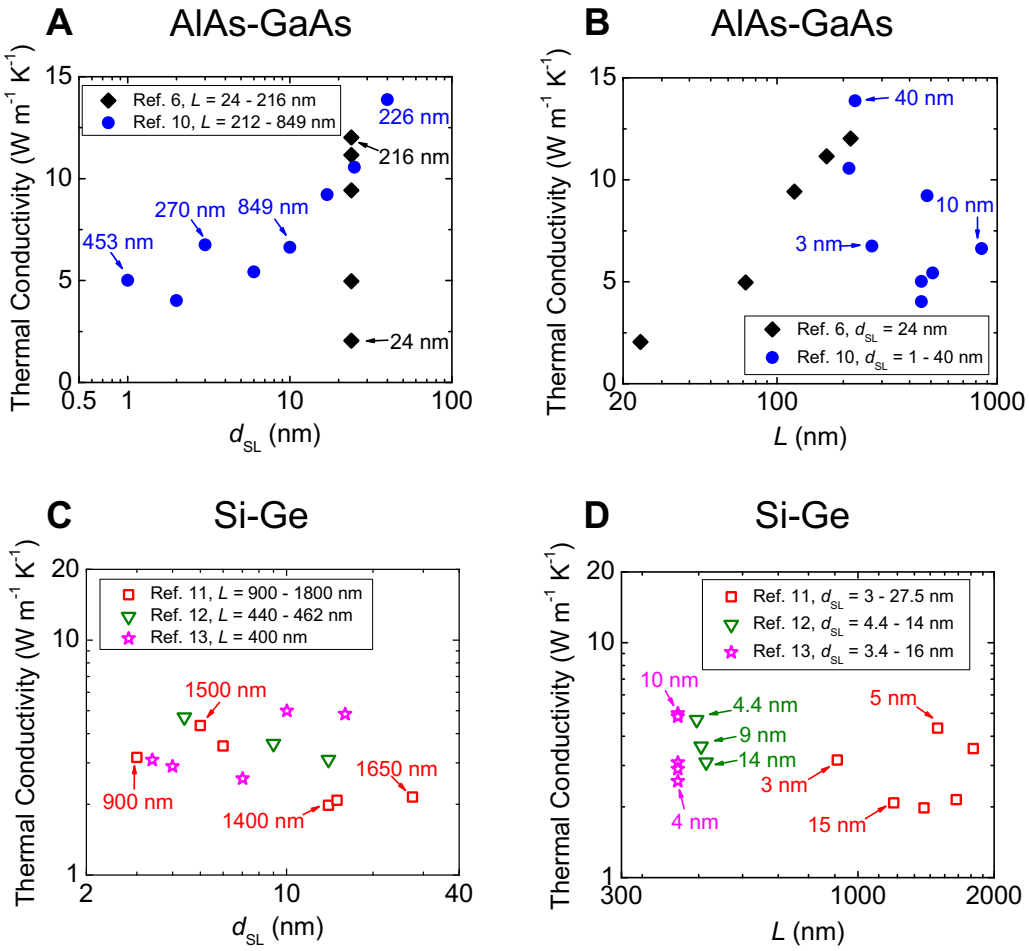

FIG. 1. Literature data of cross-plane thermal conductivities of AlAs-GaAs and Si-Ge SLs plotted versus d_{SL} in (A) and (C) and versus L in (B) and (D), respectively. Data are taken from Refs. 6 and 10 for AlAs-GaAs and Refs. 11, 12, and 13 for Si-Ge. Selected data points are labeled by the corresponding value of L in (A) and (C) and the corresponding value of d_{SL} in (B) and (D). All data are at room temperature.

mal conductivity with period thickness, Chakraborty *et al.*[13] reported a minimum in κ_{SL} at $d_{SL} = 7$ nm. The samples in these two studies had similar values of d_{SL} and L. Moreover, Lee *et al.*[11] showed no clear trend in neither d_{SL} nor L. It is worth noting that the larger discrepancy in Si-Ge superlattices could be due to the large lattice mismatch between Si and Ge ($\sim 4\%$), and thus, the AlAs and GaAs SL system, which exhibits a lattice mismatch of $\sim 0.2\%$, is a better suited material system to study the physics of phonon thermal transport across periodic structures.

Based on previous studies, no conclusive trend in the dependence of thermal conductivity on d_{SL} or L can be drawn. As a result, the interplay between short and long range boundary scattering is not fully understood and requires a systematic experimental study that isolates the contributions of each of these mechanisms to phononic thermal transport. Most importantly, an understanding of the interplay between these different length scales of boundary scattering is a necessity to fully elucidate the fundamental mechanisms of coherent phonon transport, as these theories are based on the trends in both period and thickness dependency of the thermal conductivity of SLs.[5–7] Currently, the experimental data that exist in the literature leaves holes in the existing understanding of nature, behavior and spectral scope of coherent transport in SLs.

In this work, we report on experimental measurements of the cross-plane thermal conductivities of three sets of AlAs-GaAs SLs of period thicknesses of 2, 12, and 24

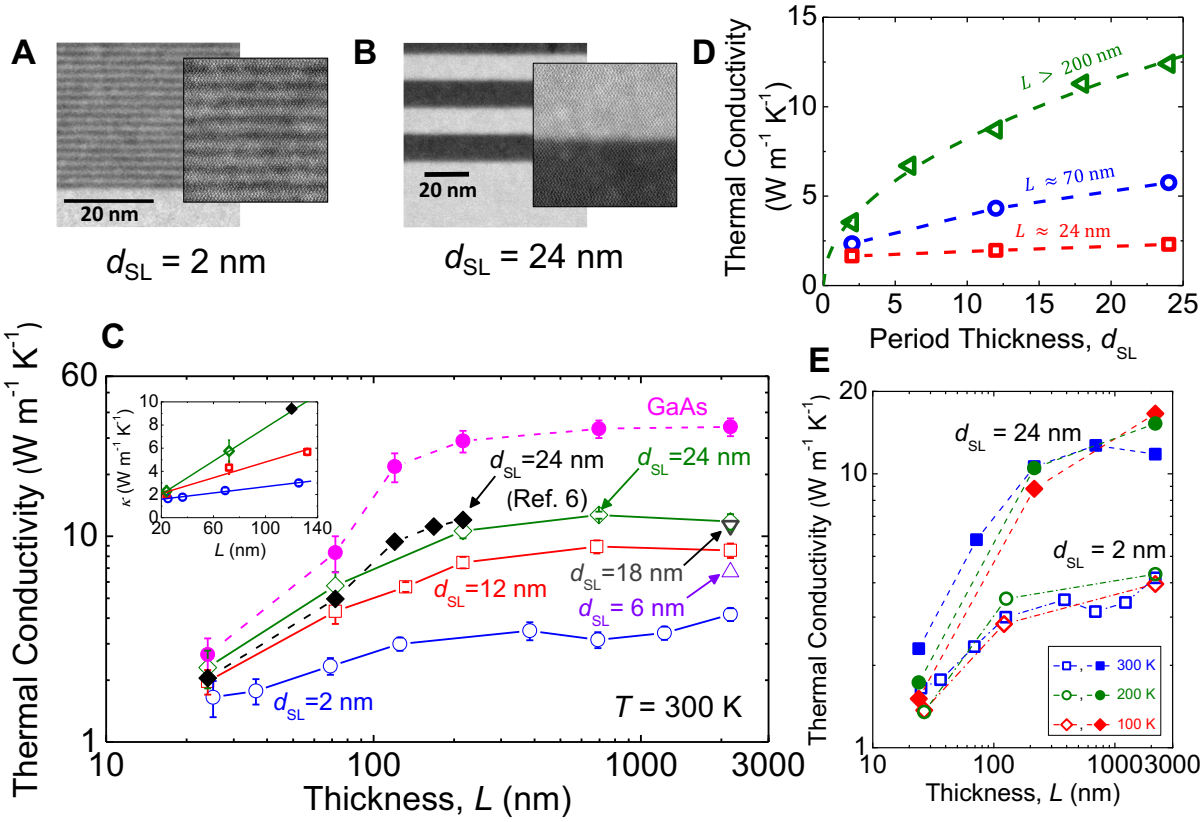

FIG. 2. (A) and (B) STEM images on two of the AlAs-GaAs SL samples. (C) Cross-plane thermal conductivity measurements on three sets of AlAs-GaAs SLs of 2, 12, and 24 nm period thicknesses and a set of thin film GaAs samples plotted versus SL thickness, L, at room temperature. The lines connecting the various data sets are guides to the eye. The figure also shows good agreement between our measurement results on samples with d_{SL} = 24 nm and those by Luckyanova *et al.*[6] The inset is a zoomed view of the data for samples with $L < 136$ nm plotted on a linear-linear scale. The solid lines in the inset are linear fits to the plotted data points. (D) Selected data from (C) plotted versus period thickness, d_{SL}. Green left triangles represent κ_{SL} in the diffusive regime obtained by taking average values of thermal conductivities of films with $L > 216$ nm for each data set d_{SL} = 2, 12, and 24 nm and the two data points at L = 2,160 nm for d_{SL} = 6 and 18 nm. The lines are guides to the eye. (E) Thermal conductivity as a function of SL thickness, L, at three different temperatures (100 and 200 K compared to room temperature). The trend at low temperatures is similar to that at room temperature suggesting that the mechanisms of heat transfer are dictated by the sample geometry even though the characteristic length and the mean free path distribution of heat carriers are significantly altered.

nm with varying sample thicknesses ranging from 20.1 to 2,160 nm and a 50:50 volume fraction. In this way, we systematically create a mesh of superlattices with varying L and d_{SL} values over which the thermal conductivity is measured. Our experimental results demonstrate the existence of classical size effects in SLs, even at the highest interface density samples. To understand the contributions of coherent and incoherent phonon transport in the regime where κ_{SL} varies quasi-linearly with L, we perform harmonic non-equilibrium Green's function calculations. Our analysis suggests that the observation of a linear-like increase in thermal conductivity as a function of SL thickness, L, could have significant contributions from incoherent phonon transport. This work demonstrates the importance of studying both period and sample thickness dependencies of thermal conductivity to understand the relative contributions of coherent and incoherent phonon transport in the thermal conductivity of SLs.

II. EXPERIMENTAL RESULTS

Samples were grown using molecular beam epitaxy (MBE). It has been shown that MBE produces interfaces between AlAs and GaAs that exhibit up to three monolayer wide interfacial mixing layer.[18] Figures 2A and 2B show scanning transmission electron microscope (STEM) images of two of the superlattice samples confirming a high interface quality. In general, an intermixing layer of

the order of ∼1 nm is observed with the initial few monolayers showing strong intermixing and subsequent layers showing reduced intermixing. Details of sample growth and thermal measurements are given in the Supplemental Material.[17]

Cross-plane thermal conductivities at room temperature, measured with time-domain thermoreflectance[19–21] (details in the Supplemental Material),[17] are plotted versus L in Fig. 2C and versus d_{SL} in Fig. 2D. For the three different period thickness sample sets, the thermal conductivity increases quasi-linearly with L followed by a plateau for thickness larger than ∼200 nm. A linear slope indicates ballistic phonon transport, or phonon flow without momentum backscattering within the sample. In this case, phonon scattering comes only from the boundaries of the sample. A plateau indicates diffusive transport, or flow dictated by phonon scattering within the sample. The dependence of κ_{SL} on L for $L < 200$ nm demonstrates the existence of long-range boundary scattering, or classical size effects,[22] even in the SLs with highest interface density ($d_{SL} = 2$ nm). This is also apparent by examining the trends in κ_{SL} vs. d_{SL} for the thinnest samples ($L \approx 24$ nm) in Fig. 2D. For this sample thickness, κ_{SL} becomes nearly independent of d_{SL}, and is thus limited by scattering at the sample boundary (L) and not the period boundaries spaced by d_{SL}. This is a clear indication of quasi-ballistic transport. The transition from quasi-ballistic to diffusive transport takes place when the effective mfp becomes comparable to the total thickness and phonons diffusively scatter within the SL instead of at the SL-substrate interface. We note that these trends in κ_{SL} vs. L are similar at lower temperatures also, as shown in Fig. 2E, suggesting that the mechanisms of heat transfer are dictated by the sample geometry even though the characteristic length and the mean free path distribution of heat carriers are altered.

The ballistic-diffusive transition is also present in the thermal conductivity data of thin film GaAs (Fig. 2C). The fact that this transition occurs at nearly the same thickness of the SL films, for all values of d_{SL}, and the same thickness of the GaAs films suggests that boundary scattering of long mfp (low frequency) phonons at the film/substrate interface is limiting thermal transport in these structures.[9] The inclusion of interfaces via SLs impedes short mfp phonons leading to a reduction in the magnitude of thermal conductivity of SLs as compared to thin film GaAs.

III. DISCUSSION AND MODELING: COHERENT VS. INCOHERENT EFFECTS

Several works on thermal transport in SLs reported a minimum in κ_{SL} as a function of d_{SL} that denotes a crossover from coherent transport (wavelike) at short d_{SL} to incoherent transport (particlelike) at larger d_{SL}.[5,7,13,23–38] We are not aware of a systematic study of the dependence of κ_{SL} on both d_{SL} and L in these previous works. Furthermore, a range of different interpretations for the existence or absence of a minimum have been posed. The most common interpretation explains the minimum as a product of the competition between the reduction in phonon group velocity due to miniband formation at short period thicknesses and the increase in the total phonon lifetimes as the period thickness increases.[7,30,39] The absence of the minimum has been attributed to interfacial defects,[24,25,28] large lattice mismatch between the SL constituent materials,[27] short phonon coherence length as compared to d_{SL},[5,31] dominance of anharmonic scattering processes,[5,27] or periodicity disorder as in random multilayers[33,34] and quasi-periodic SLs.[32,35] These different factors destroy wave coherence increasing the relative contribution of incoherent phonons to thermal transport. This increased role of particle-like phonons dictates the increasing trend in κ_{SL} versus d_{SL} over the opposite trend produced by coherent phonons. Our data shows only an increasing trend of κ_{SL} versus d_{SL} (Fig. 2D). The absence of a minimum from our data on AlAs-GaAs SLs can be explained in terms of the short phonon coherence length, which was previously estimated to be of the order of one nanometer for bulk GaAs.[5,40] In addition, the existence of interfacial mixing layer can mask the minimum in κ_{SL}.[16,30,41–43]

In the light of the several literature reports and the trend in our data shown in Fig. 2D, one could posit that the change in κ_{SL} with d_{SL} is driven by incoherent phonons that are not dictated by miniband formation. However, Luckyanova *et al.*[6] recently interpreted the linear dependence of κ_{SL} on L, an indicator of ballistic transport, as a proof that coherent phonons dominate heat conduction in AlAs-GaAs SLs of $d_{SL} = 24$ nm and $L = 24-216$ nm. Luckyanova suggested that in the ballistic regime, phonon conductance and transmission remain constant even though more interfaces are added to the sample as its length increases. This is only possible if phonons preserve their phase information as they propagate through the internal interfaces. As a result, they "see" the SL as a new homogeneous material and their transport properties are governed by miniband formation in the dispersion curve. Our data suggest that although coherent phonon transport could contribute to the linear dependence of κ_{SL} on L (for $L < 200$ nm), the variation of κ_{SL} with d_{SL} is driven by incoherent phonons, even thought phonon transport through the SL is still quasi-ballistic.

To further substantiate the findings from the experimental results presented in Figs. 2C and 2D, we calculate the thermal conductance of GaAs-AlAs SL using a harmonic Atomistic Green's functions (GF) analysis, which naturally accounts for coherent effects in phonon transport (including miniband formation), unlike semi-classical Kinetic Theory-based models, which require pre-assumed input to calculate coherent effects on κ_{SL} (see the Supplemental Material[17] for discussion of Kinetic Theory-based[44,45] and Boltzmann Transport Equation-based[46–50] modeling of phonon transport in the

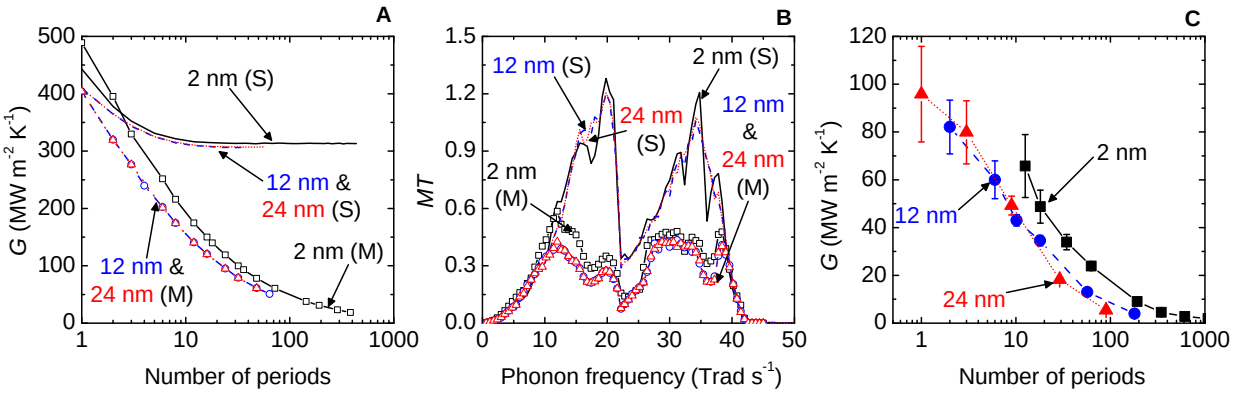

FIG. 3. (A) Conductance vs. number of periods for SL with atomically smooth "(S)" and mixed "(M)" interfaces. The decrease in conductance on the SLs with interatomic mixing at the interfaces results from incoherent phonon transport. (B) $M\mathcal{T}$ per perpendicular unit cell for SL with atomically smooth "(S)" and mixed "(M)" interfaces. The decrease in $M\mathcal{T}$ as the number of periods increases show the corresponding decrease in transmission, which signal incoherent phonon transport. For these calculations, the total sample thickness is set to 12 periods of AlAs-GaAs for each sample regardless of the period. (C) Experimental data replotted as conductance vs number of periods. The data shows that conductance is independent of period for short samples with long periods.

AlAs-GaAs SLs, including modeling validation with existing bulk thermal conductivity data,[44,51–54] determining spectral phonon scattering rates using DFT,[47,48,55] and estimates for the thermal conductivity accumulation and spectral mean free paths of the phonons in the AlAs-GaAs SLs based on Kinetic Theory modeling[55,56]). Within this Atomistic Green's function formalism, the conductance is given by[57–59]

$$G = \frac{1}{A}\int_0^\infty \frac{d\omega}{2\pi}\hbar\omega\frac{\partial f}{\partial T}M\mathcal{T} \approx \frac{k_B}{2\pi A}\int_0^\infty d\omega M\mathcal{T}, \quad (1)$$

with $\hbar\omega$ the phonon energy, k_B the Boltzmann constant, f the Bose-Einstein distribution, T the temperature and $M\mathcal{T}$ the sum of all the transmissions over all of the phonon modes from a left-contact to a right-contact. For the simulations presented here, the interatomic force constants for GaAs and AlAs were calculated from Density Functional Perturbation Theory using Quantum Espresso.[60,61] Note that at $T = 300$ K, the heat capacity per mode is nearly constant ($\hbar\omega\partial f/\partial T \approx k_B$) over the available phonon spectrum, and thus the conductance is approximately proportional to the area under $M\mathcal{T}$ (Eq. 1). Details of the calculations are given in the Supplemental Material,[17] and we note that we have benchmarked our GF algorithms against various previous works in the literature, including those simulating random interatomic mixing at interfaces, as described in our previous works.[62,63]

To explore the contribution of coherent phonon transport on the thermal conductance, we simulate SLs with perfect interfaces and SLs with interatomic mixing at the interfaces. Phonon transport is fully coherent for the SLs with perfect interfaces due to the construction of the GF method. On the other hand, the stochasticity of the interatomic mixing at the interfaces creates spatial incoherence. This type of incoherence is captured by our GF simulations when we average the transmission over several purely coherent simulations of independent SL with different random mixing at the interfaces.[64]

When the SLs have perfect interfaces and phonon transport is purely coherent, the conductance across the SL initially decreases and then levels off as the thickness of the SL increases (Fig. 3A). This leveling off of the conductance is a direct consequence of coherent phonon transport, since the conductance does not decrease in spite of increasing the number of interfacial scattering centers, consistent with the discussions in Ref. 6. The initial decrease in the conductance results from the decrease of the transmission of SL phonons that are evanescent in a infinitely long superlattice. Those phonons do not fully decay in a SL with a few periods because interference is not strong enough at these length scales. Figure 3A also shows that the conductance is independent of the period thickness for the SL with 12 nm and 24 nm period (for periods larger than ~ 4 nm, assuming perfect interfaces).

Even in the absence of phonon-phonon interactions, when random interatomic mixing is added at the interfaces, incoherent phonon transport becomes increasingly important as the number of interfaces increases. Our simulations show that both the conductance, G, and transmission, $M\mathcal{T}$, decrease monotonically as the number of periods increases (Fig. 3A and Supplemental Fig. 5 in the

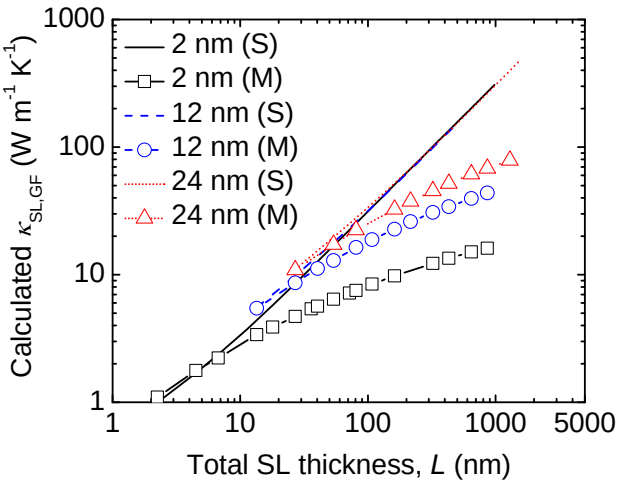

FIG. 4. Thermal conductivity of AlAs-GaAs SLs calculated via our Green's function analysis ($\kappa_{SL,GF}$) vs. number of periods for SLs with atomically smooth "(S)" and mixed "(M)" interfaces. For SLs with perfect interfaces, the slope is nearly independent of the period. For SLs with mixed interfaces, the slope seems linear in spite of incoherent phonon transport. We note that this calculated value for $\kappa_{SL,GF}$ does not include phonon-phonon interactions.

Supplemental Material,[17] respectively). Since the conductance does not become constant after a few periods, most of the phonons never "see" the SL as a new homogeneous material and heat conduction cannot be completely coherent. Instead, as the number of interfaces increases, transmission decreases rapidly and incoherent transport becomes the dominant effect.

Our simulations of phonon transport in the SLs with mixing at the interfaces suggest that the conductance depends on the number of periods in the sample but not on the period itself, as long as the period is larger than 4 nm (note, as previously mentioned, our simulations do not account for phonon-phonon interactions). Figure 3B shows that $M\mathcal{T}$ for SLs with period thicknesses of 12 nm (6 nm AlAs-6 nm GaAs) and 24 nm (12 nm AlAs-12 nm GaAs) are the same when the number of periods of the samples are equal, which follows from the lack of scattering in between interfaces in our simulations. Our experimental data confirms this result for samples shorter than 100 nm as the conductance of the 24 nm and 12 nm period samples follow a single curve (Fig. 3C); note, these experimental trends are qualitatively well captured by our simulations with interatomic mixing in Fig. 3A. The dependency of the conductance only on the number of periods for samples shorter than 100 nm, implies that conductance is not independent of length since longer samples with more periods have less conductance (Fig. 3C). This also explains the experimentally observed increase in the slope of κ vs. L from the 12 nm period to the 24 nm period sample. At a given length, the 24 nm period samples have half the number of periods of the 12 nm period sample. This translates to a larger $M\mathcal{T}$, a larger conductance, and thus a larger slope in κ.

It is interesting to note that the conductances of the 2 nm period samples are higher than that of the 24 and 12 nm samples (Fig. 3A and C). We hypothesize that this increase is due to a transition to alloy-like behavior in phonon transport for the 2 nm period SLs, which is supported due to the few monolayers of compositional mixing that we observed in all of our samples around the AlAs-GaAs interfaces. Our simulations suggest this is not due to coherent miniband formation,[5,7,39] since the features of $M\mathcal{T}$ for the 2 nm period SLs with and without interatomic mixing at the interfaces have different features (Fig. 3B).

Our GF analysis suggests that a seemingly linear slope in κ vs. L may actually contain important contributions from incoherent phonon transport. This linear slope in κ vs L, which has been ascribed to coherent phonon transport,[6] may actually be non-linear when extended to a larger number of periods, which is a signature of incoherent effects. We show these GF results in Fig. 4, where we plot the GF-simulated thermal conductivity of various SLs ($\kappa_{SL,GF}$) with atomically smooth "(S)" and mixed "(M)" interfaces as a function of total SL thickness, L. Note, this calculated value of $\kappa_{SL,GF}$ does not include phonon-phonon interactions. As shown in Fig. 4, the trend in $\kappa_{SL,GF}$ vs L for superlattices with interatomic mixing at the interfaces could easily be interpreted as linear when the number of period is small. Nevertheless, the calculated transmission, $M\mathcal{T}$, of these "mixed" SL show a strong decay of the phonon transmission as the number of periods increases, which suggests incoherent contributions to phonon transport.

IV. SUMMARY

In summary, we presented thermal conductivity measurements on AlAs-GaAs SLs with at wide range of sample thicknesses and period thicknesses. These results demonstrate the existence of classical size effects in SLs even at the highest interface density samples. Coupled with harmonic Green's function calculations, our results suggest that the observation of a quasilinear increase in thermal conductivity can have important contributions from incoherent phonon transport, even through the transport is still in the ballistic regime. This work demonstrates the importance of studying both period and sample thickness dependencies of thermal conductivity to understand the relative contributions of coherent and incoherent phonon transport in the thermal conductivity in SLs.

ACKNOWLEDGMENTS

This material is based upon work supported by the Air Force Office of Scientific Research under Award No. FA9550-15-1-0079.

* To whom correspondence should be addressed. E-mail: phopkins@virginia.edu

[1] I. Chowdhury, R. Prasher, K. Lofgreen, G. Chrysler, S. Narasimhan, R. Mahajan, D. Koester, R. Alley, and R. Venkatasubramanian, Nature Nanotechnology **4**, 235 (2009).

[2] A. Shakouri, Proceedings of the IEEE **94**, 1613 (2006).

[3] B. S. Williams, Nature photonics **1**, 517 (2007).

[4] G. Chen, C. L. Tien, X. Wu, and J. S. Smith, Journal of Heat Transfer **116**, 325 (1994).

[5] J. Ravichandran, A. K. Yadav, R. Cheaito, P. B. Rossen, A. Soukiassian, S. Suresha, J. C. Duda, B. M. Foley, C.-H. Lee, Y. Zhu, *et al.*, Nature Materials **13**, 168 (2014).

[6] M. N. Luckyanova, J. Garg, K. Esfarjani, A. Jandl, M. T. Bulsara, A. J. Schmidt, A. J. Minnich, S. Chen, M. S. Dresselhaus, Z. Ren, E. A. Fitzgerald, and G. Chen, Science **338**, 936 (2012).

[7] M. V. Simkin and G. D. Mahan, Physical Review Letters **84**, 927 (2000).

[8] Y. K. Koh, Y. Cao, D. G. Cahill, and D. Jena, Advanced Functional Materials **19**, 610 (2009).

[9] R. Cheaito, J. C. Duda, T. E. Beechem, K. Hattar, J. F. Ihlefeld, D. L. Medlin, M. A. Rodriguez, M. J. Campion, E. S. Piekos, and P. E. Hopkins, Physical Review Letters **109**, 195901 (2012).

[10] W. S. Capinski, H. J. Maris, T. Ruf, M. Cardona, K. Ploog, and D. S. Katzer, Physical Review B **59**, 8105 (1999).

[11] S.-M. Lee, D. G. Cahill, and R. Venkatasubramanian, Applied Physics Letters **70**, 2957 (1997).

[12] T. Borca-Tasciuc, W. Liu, J. Liu, T. Zeng, D. W. Song, C. D. Moore, G. Chen, K. L. Wang, M. S. Goorsky, T. Radetic, R. Gronsky, T. Koga, and M. S. Dresselhaus, Superlattices and Microstructures **28**, 199 (2000).

[13] S. Chakraborty, C. A. Kleint, A. Heinrich, C. M. Schneider, J. Schumann, M. Falke, and S. Teichert, Applied Physics Letters **83**, 4184 (2003).

[14] T. Yao, Applied Physics Letters **51**, 1798 (1987).

[15] X. Y. Yu, G. Chen, A. Verma, and J. S. Smith, Applied Physics Letters **67**, 3554 (1995).

[16] M. N. Luckyanova, J. A. Johnson, A. Maznev, J. Garg, A. Jandl, M. T. Bulsara, E. A. Fitzgerald, K. A. Nelson, and G. Chen, Nano Letters **13**, 3973 (2013).

[17] See Supplemental Material at [URL will be inserted by publisher] for details on sample growth, time domain thermoreflectance (TDTR), thermal conductivity data and experimental data analysis, Atomistic Green's function analysis of coherent transport and incoherent transport at mixed interfaces, density functional theory applied to GaAs and AlAs, and modeling the spectral phonon contributions to the thermal conductivity in AlAl-GaAs superlattice.

[18] P. D. Robb and A. J. Craven, Ultramicroscopy **109**, 61 (2008).

[19] D. G. Cahill, Review of Scientific Instruments **75**, 5119 (2004).

[20] A. J. Schmidt, X. Chen, and G. Chen, Review of Scientific Instruments **79**, 114902 (2008).

[21] P. E. Hopkins, J. R. Serrano, L. M. Phinney, S. P. Kearney, T. W. Grasser, and C. T. Harris, Journal of Heat Transfer **132**, 081302 (2010).

[22] H. Casimir, Physica **5**, 495 (1938).

[23] R. Venkatasubramanian, Physical Review B **61**, 3091 (2000).

[24] B. C. Daly, H. J. Maris, K. Imamura, and S. Tamura, Physical Review B **66**, 024301 (2002).

[25] K. Imamura, Y. Tanaka, N. Nishiguchi, S. Tamura, and H. Maris, Journal of Physics: Condensed Matter **15**, 8679 (2003).

[26] B. Yang and G. Chen, Phys. Rev. B **67**, 195311 (2003).

[27] Y. Chen, D. Li, J. R. Lukes, Z. Ni, and M. Chen, Physical Review B **72**, 174302 (2005).

[28] E. S. Landry and A. J. H. McGaughey, Physical Review B **79**, 075316 (2009).

[29] K.-H. Lin and A. Strachan, Physical Review B **87**, 115302 (2013).

[30] J. Garg and G. Chen, Physical Review B **87**, 140302 (2013).

[31] B. Latour, S. Volz, and Y. Chalopin, Physical Review B **90**, 014307 (2014).

[32] T. Zhu and E. Ertekin, Phys. Rev. B **90**, 195209 (2014).

[33] Y. Wang, H. Huang, and X. Ruan, Phys. Rev. B **90**, 165406 (2014).

[34] Y. Wang, C. Gu, and X. Ruan, Applied Physics Letters **106**, 073104 (2015), 10.1063/1.4913319.

[35] X. Mu, T. Zhang, D. B. Go, and T. Luo, Carbon **83**, 208 (2015).

[36] W. Li, X. Chen, Z. Zheng, and Y. Chen, Computational Materials Science **112, Part A**, 107 (2016).

[37] C. da Silva, F. Saiz, D. A. Romero, and C. H. Amon, Phys. Rev. B **93**, 125427 (2016).

[38] B. Saha, Y. R. Koh, J. Comparan, S. Sadasivam, J. L. Schroeder, M. Garbrecht, A. Mohammed, J. Birch, T. Fisher, A. Shakouri, and T. D. Sands, Phys. Rev. B **93**, 045311 (2016).

[39] S. Y. Ren and J. D. Dow, Physical Review B **25**, 3750 (1982).

[40] G. Chen, Journal of Heat Transfer **119**, 220 (1997).

[41] Z. Tian, K. Esfarjani, and G. Chen, Physical Review B **86**, 235304 (2012).

[42] S. P. Hepplestone and G. P. Srivastava, Physical Review B **82**, 144303 (2010).

[43] C.-W. Wu and Y.-R. Wu, AIP Advances **6**, 115201 (2016), https://doi.org/10.1063/1.4967202.

[44] M. G. Holland, Physical Review **134**, A471 (1964).

[45] J. Callaway, Physical Review **113**, 1046 (1959).

[46] W. Li, J. Carrete, N. A. Katcho, and N. Mingo, Computer Physics Communications **185**, 1747 (2014).

[47] A. Ward, D. A. Broido, D. A. Stewart, and G. Deinzer, Physical Review B **80**, 125203 (2009).

[48] A. Ward and D. A. Broido, Physical Review B **81**, 085205 (2010).

[49] M. Omini and A. Sparavigna, Physica B: Condensed Matter **212**, 101 (1995).

[50] M. Omini and A. Sparavigna, Physical Review B **53**, 9064 (1996).

[51] S. Adachi, *Properties of Aluminium Gallium Arsenide* (The Institution of Engineering and Technology, 1993).

[52] M. Abrahams, R. Braunstein, and F. Rosi, Journal of Physics and Chemistry of Solids **10**, 204 (1959).

[53] R. O. Carlson, G. A. Slack, and S. J. Silverman, Journal of Applied Physics **36**, 505 (1965).

[54] M. A. Afromowitz, Journal of Applied Physics **44**, 1292 (1973).

[55] T. Luo, J. Garg, J. Shiomi, K. Esfarjani, and G. Chen, EPL (Europhysics Letters) **101**, 16001 (2013).

[56] F. Yang and C. Dames, Physical Review B **87**, 035437 (2013).

[57] N. Mingo and L. Yang, Physical Review B **68**, 245406 (2003).

[58] S. Datta, *Quantum Transport: Atom to Transistor*, 2nd ed. (Cambridge University Press, 2005).

[59] J.-S. Wang, J. Wang, and J. T. Lü, The European Physical Journal B **62**, 381 (2008).

[60] P. Giannozzi, S. Baroni, N. Bonini, M. Calandra, R. Car, C. Cavazzoni, D. Ceresoli, G. L. Chiarotti, M. Cococcioni, I. Dabo, A. Dal Corso, S. de Gironcoli, S. Fabris, G. Fratesi, R. Gebauer, U. Gerstmann, C. Gougoussis, A. Kokalj, M. Lazzeri, L. Martin-Samos, N. Marzari, F. Mauri, R. Mazzarello, S. Paolini, A. Pasquarello, L. Paulatto, C. Sbraccia, S. Scandolo, G. Sclauzero, A. P. Seitsonen, A. Smogunov, P. Umari, and R. M. Wentzcovitch, Journal of physics. Condensed matter : an Institute of Physics journal **21**, 395502 (2009).

[61] S. Baroni, S. De Gironcoli, A. Dal Corso, and P. Giannozzi, Reviews of Modern Physics **73**, 515 (2001).

[62] C. A. Polanco, R. Rastgarkafshgarkolaei, J. Zhang, N. Q. Le, P. M. Norris, P. E. Hopkins, and A. W. Ghosh, Physical Review B **92**, 144302 (2015).

[63] C. A. Polanco, R. Rastgarkafshgarkolaei, J. Zhang, N. Q. Le, P. M. Norris, and A. W. Ghosh, Physical Review B **95**, 195303 (2017).

[64] A. Ghosh, *Nanoelectronics: A Molecular View* (World Scientific Publishing Co. Pte. Ltd., Hackensack, NJ, 2017).